Internal Report: Numerical predictions of several configurations of circular cylinders

N. M. NIGRO, R. R. PAZ, G. FILIPPINI and M. A. STORTI

Centro Internacional de Métodos Computacionales en Ingeniería (CIMEC)
CONICET - INTEC - U.N.L.
Güemes 3450, (3000) Santa Fe, Argentina

SUMMARY

In this paper, the accuracy of the numerical predictions of flow around several cofigurations of circular cylinders is analyzed. The discretization of partial differential equations arising in the context of this incompressible CFD problem is done by means of the Finite Element Method implemented in a parallel code running on a Beowulf Cluster of PC developed at CIMEC laboratory (`http://www.cimec.org.ar/petscfem`). Comparison of drag and lift forces and also the Strouhal number for both a single cylinder and for differents configurations of the circular cylinders against other numerical results published earlier and also against experimental observations are included. Some conclusions about the importance of solving some 3D vortex shedding structures to fit experimental observations and numerical results are addressed.

KEY WORDS: staggered circular cylinders, computational fluid dynamics, parallel computing

1. INTRODUCTION

Fluid flow around a circular cylinder is a classical problem in fluid mechanics where in general a lot of experimental measurements are available and also for low Reynolds numbers is possible to get some analytical solutions. This fact had pushed to CFD community to use this test as a benchmark to validate CFD code development.

It is very common to sweep the experiment for a wide range of Reynolds numbers trying to capture some different flow patterns, specially the drag crisis arising at approximately a Reynolds number of 100000. For this test case the most of the numerical predictions are done in a two dimensional geometry arguing that for very wide circular cylinders the 3D flow structures are only concentrated at the ends.

*Correspondence to: N. N. Nigro, Centro Internacional de Métodos Computacionales en Ingeniería (CIMEC). Güemes 3450, (3000) Santa Fe, Argentina.
E-mail: nnigro@intec.unl.edu.ar

Numerical solutions in general show a very good agreement for very low Reynolds numbers, loosing this good fitness at medium Reynolds numbers and finally returning to have an acceptable solution for high Reynolds numbers with very fine meshes.

Recently, some researchers ([13, 12]) had shown that this lack of adjustment at medium Reynolds numbers is caused by the unresolved spanwise vortex shedding structures that appear at Reynolds numbers close to 200 and were identified as A mode and B mode.

Here enclosed some brief summary of the conclusions of Balachandar in his paper:

It has been known for some time that two-dimensional numerical simulations of flow over nominally two-dimensional bluff bodies at Reynolds numbers for which the flow is intrinsically three dimensional, lead to inaccurate prediction of the lift and drag forces. In particular, for flow past a normal flat plate (International Symposium on Nonsteady Fluid Dynamics, edited by J. A. Miller and D. P. Telionis, 1990, pp. 455b circular cylinders [J. Wind Eng. Indus. Aerodyn. 35, 275 (1990)], it has been noted that the drag coefficient computed from two-dimensional simulations is significantly higher than what is obtained from experiments. Furthermore, it has been found that three-dimensional simulations of flows lead to accurate prediction of drag [J. Wind Eng. Indus. Aerodyn. 35, 275 (1990)]. The underlying cause for this discrepancy is that the surface pressure distribution obtained from two-dimensional simulations does not match up with that obtained from experiments and three-dimensional simulations and a number of reasons have been put forward to explain this discrepancy. However, the details of the physical mechanisms that ultimately lead to the inaccurate prediction of surface pressure and consequently the lift and drag, are still not clear. In the present study, results of two-dimensional and three-dimensional simulations of flow past elliptic and circular cylinders have been systematically compared in an effort to pinpoint the exact cause for the inaccurate prediction of the lift and drag by two-dimensional simulations. The overprediction of mean drag force in two-dimensional simulations is directly traced to higher Reynolds stresses in the wake. It is also found that the discrepancy in the drag between two-dimensional and three-dimensional simulations is more pronounced for bluffer cylinders. Finally, the current study also provides a detailed view of how the fluctuation, which are associated with the Kármán vortex shedding in the wake, affect the mean pressure distribution and the aerodynamic forces on the body.

A lot of real world applications are composed by one or more cylinders in a staggered configuration with fluid flow getting through them, tall chimneys exposed to atmospheric boundary layer flows, cooling systems, bridge structures over rivers, and many others. The interference of the cylinder among them produce very complex vortex shedding structures that alter the drag and lift forces of the isolated cylinders becoming as a good strategy to control these forces. Moreover the understanding of this complex flow pattern is very important to study the mechanism of heat transfer in order to optimize the thermal efficiency of some equipments. Therefore a good comprehensive study of this fluid flow problem solved by numerical methods is neccesary to get good predictions and better design improvements.

The aim of this report is to evaluate the matching between numerical predictions against laboratory measurements, and to evaluate the possible causes of disagreement.

Mathematical aspects have been ommited for brevity reasons. Next sections include the results obtained for each case analyzed. First single cylinder results are included and finally two cylinder flow are presented.

2. NUMERICAL SOLUTIONS OF DIFERENT CONFIGURATIONS OF FLOW AROUND STAGGERED CIRCULAR CYLINDERS

In this section several numerical solutions of flow around staggered circular cylinders are presented. Basically 2D and 3D solutions were performed for single and multiple cylinders, with and without shear flow in the free stream.

The Reynolds and Strouhal numbers are based on the cylinder diameter and free stream flow parameters ($\rho_\infty = 1, U_\infty = 1$) as follows:

$$\begin{aligned} Re &= \frac{\rho_\infty ||\mathbf{u}_\infty|| D}{\mu} \\ St &= \frac{Df}{||\mathbf{u}_\infty||} \end{aligned} \tag{1}$$

The viscosity μ is adjusted in order to satisfy the Reynolds numbers of each example and f is the frequency of the lift force time history.

3. FLOW AROUND A SINGLE CIRCULAR CYLINDER

In this section the standard 2D flow around a single circular cylinder without shear flow in the free stream at several Reynolds numbers are included. Next, 2D flow around a single circular cylinder with a shear flow in the free stream at a Reynolds number of 50000 is included.

This shear flow is characterized by the dimensionless number

$$K = \frac{AD}{||\mathbf{u}_\infty||} \tag{2}$$

where A is the slope of the velocity in the cross flow direction.

Each one of the next subsections show the drag (C_D) and lift (C_L) coefficients and some details about the vortex shedding structure for some time step. Finally a table showing the main flow parameters is included.

3.1. Test # 1: Single 2D cylinder without shear

The mesh used for this first example contains 67820 nodes and 119704 triangular elements. A global view of this mesh is shown in figure (1) where nodes are clustered in the vecinity of the cylinder and along the wake. A close-up of the mesh near the cylinder is depicted in figure (2) and a detail of the structured layer of quadrangular elements over the cylinder skin is plot in figure (3). These layers allow to improve the boundary layer definition.

As a summary table I shows the drag, lift and Strouhal coefficients for several Reynolds numbers tested.

3.2. $Re = 100$

This example serves as a good starting point to check the accuracy of the flow solver for one of the simplest flow conditions. The following figures show the drag and lift coefficient time

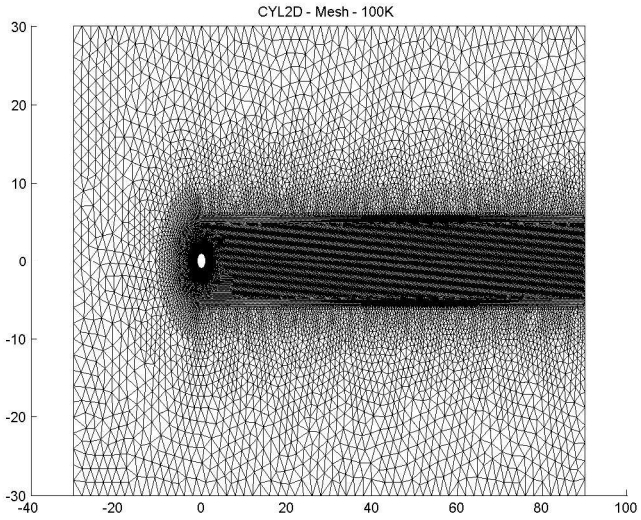

Figure 1. 2D single cylinder mesh - Global view

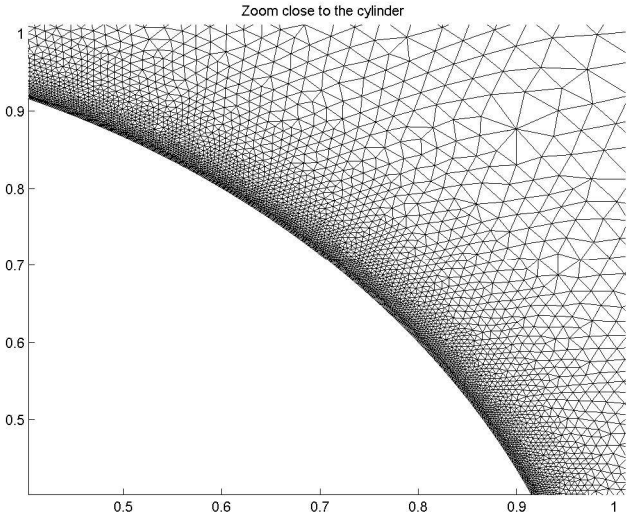

Figure 2. 2D single cylinder mesh - Zoom close to the cylinder

evolution for $Re = 100$. These values are in good agreement with other numerical results published earlier and with experimental observations.

Figure (6) shows the axial velocity for some time step where it is noticeable the well known von-Karman street in the cylinder wake.

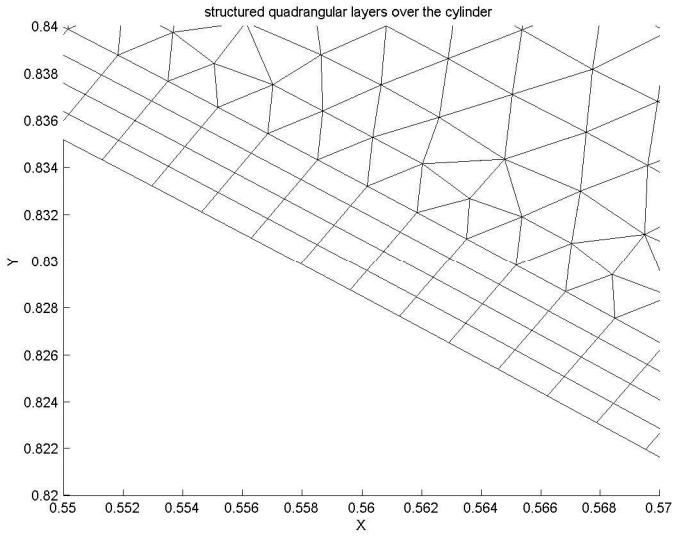

Figure 3. 2D single cylinder mesh - Structured layers around the cylinder

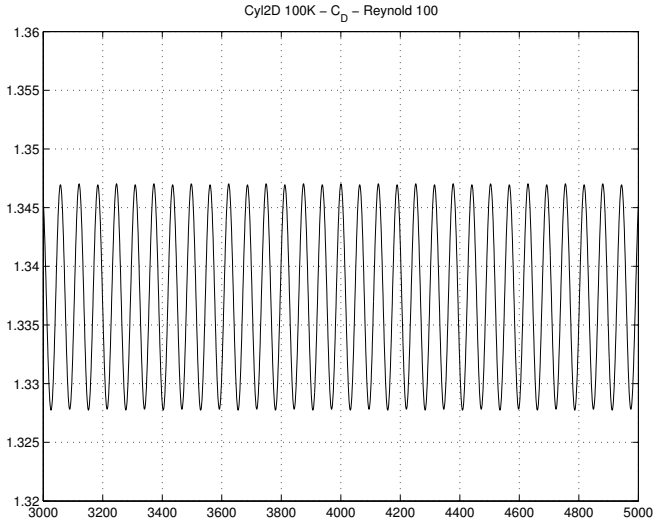

Figure 4. 2D single cylinder without shear at free stream - $Re = 100$ - Drag coefficient (C_D).

3.3. $Re = 200$

As in the first test this flow condition has a lot of bibliographic references and allow to check the validity of 2D numerical results against experimental observations. It is well known that for $Re \approx 200$ a spanwise mode appears (called mode B), that has a spatial wavelength of approximately one cylinder diameter [13].

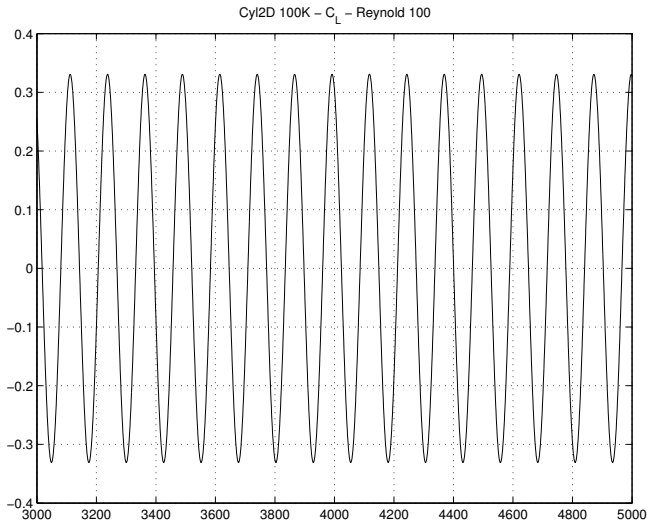

Figure 5. 2D single cylinder without shear at free stream - $Re = 100$ - Lift coefficient (C_L).

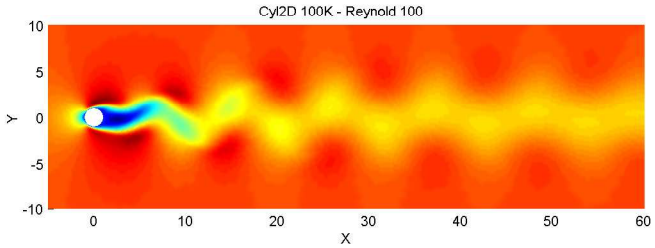

Figure 6. 2D single cylinder without shear at free stream - Axial velocity.

The following figures show the drag and lift coefficient time evolution for $Re = 200$. These values are in good agreement with other numerical results published earlier and with experimental observations.

3.4. $Re = 1000$

This flow condition evidences the separation of the numerical 2D results from the experimental measurements. One of the most strong arguments for this disagreement between numerical and experimental results is the establishment of the 3D spanwise vortex shedding structure that for this Reynolds number had changed from A-mode to B-mode [13]. The numerical drag and lift coefficients are higher than the experimental ones specially for the presence of unresolvable 3D scales at the rear region of the cylinder.

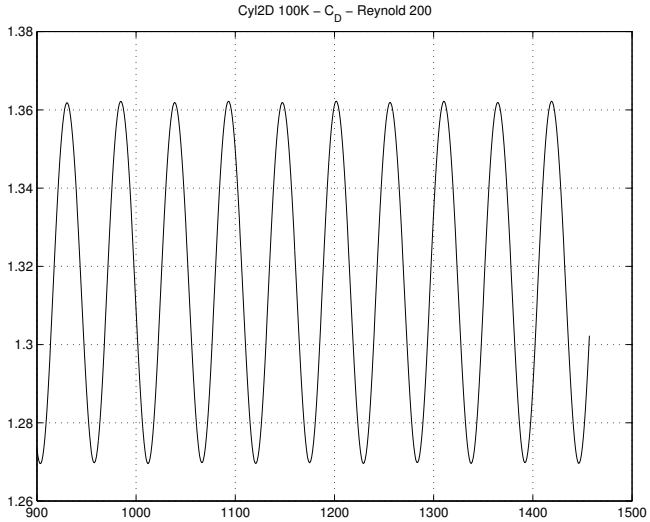

Figure 7. 2D single cylinder without shear at free stream - $Re = 200$ - Drag coefficient (C_D).

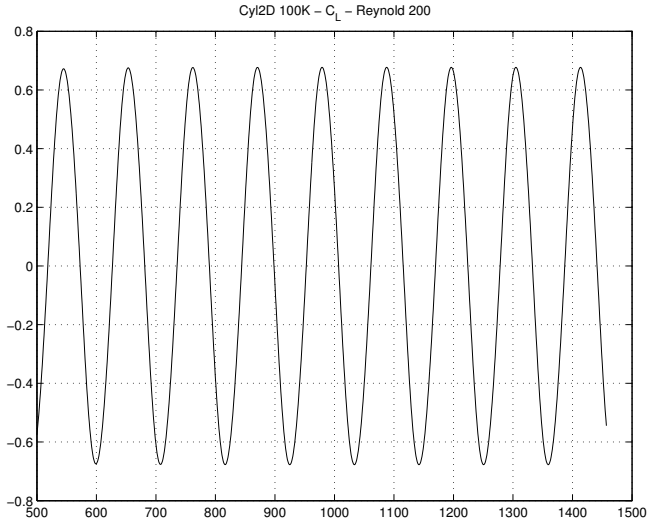

Figure 8. 2D single cylinder without shear at free stream - $Re = 200$ - Lift coefficient (C_L).

3.5. $Re = 50000$

The following plot shows the changes experimented by the cylinder wake where the von-Karman street seems to be wider and more caotic. The numerical solution becomes more irregular and the drag and lift time evolution had lost the periodic behavior with a strong coupling among several time frequencies.

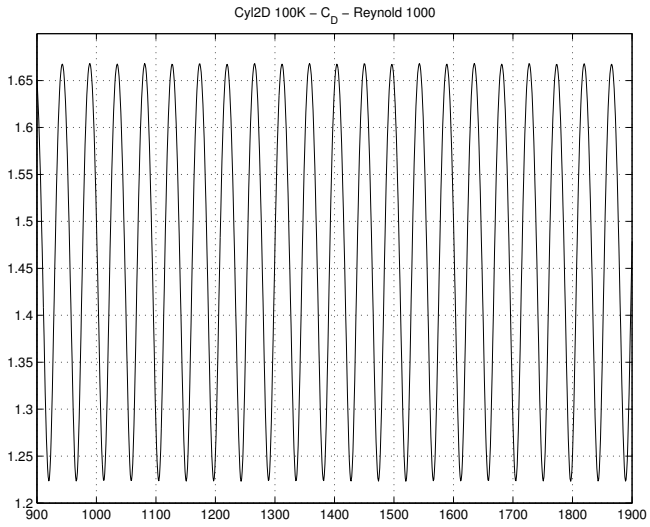

Figure 9. 2D single cylinder without shear at free stream - $Re = 1000$ - Drag coefficient (C_D).

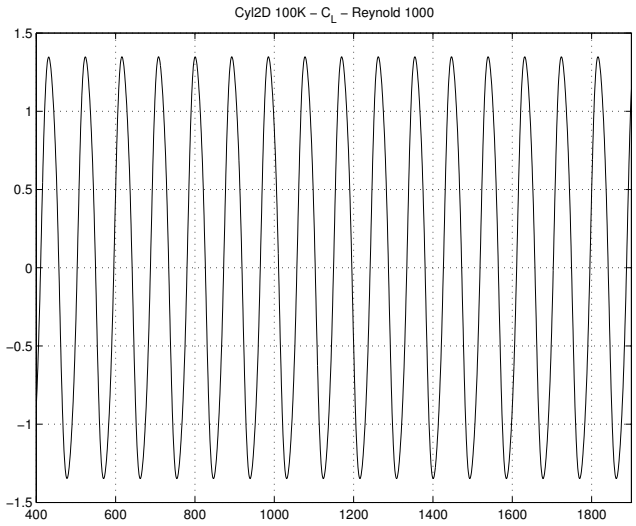

Figure 10. 2D single cylinder without shear at free stream - $Re = 1000$ - Lift coefficient (C_L).

3.6. Test # 2: Single 2D cylinder with shear - $Re = 50000$

This example show the influence of a shear flow in the incoming free stream over the drag and lift forces acting over the cylinder.

The following plot shows the von-Karman street along the cylinder wake.

The mean drag force coefficient is about 1.45 and the lift one is around -0.465.

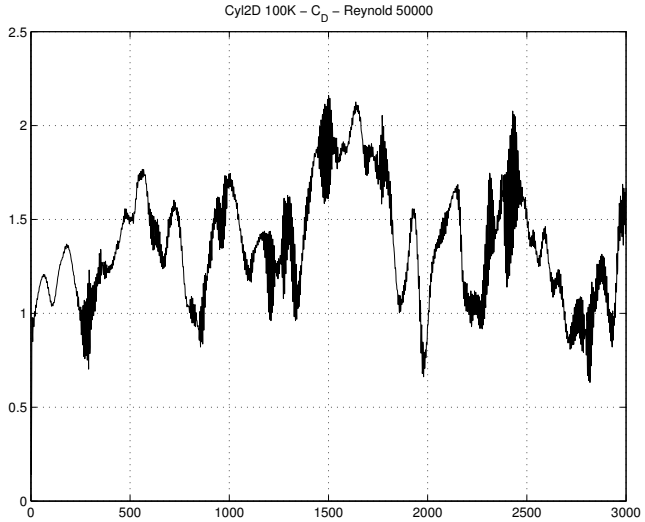

Figure 11. 2D single cylinder without shear at free stream - $Re = 50000$ - Drag coefficient (C_D).

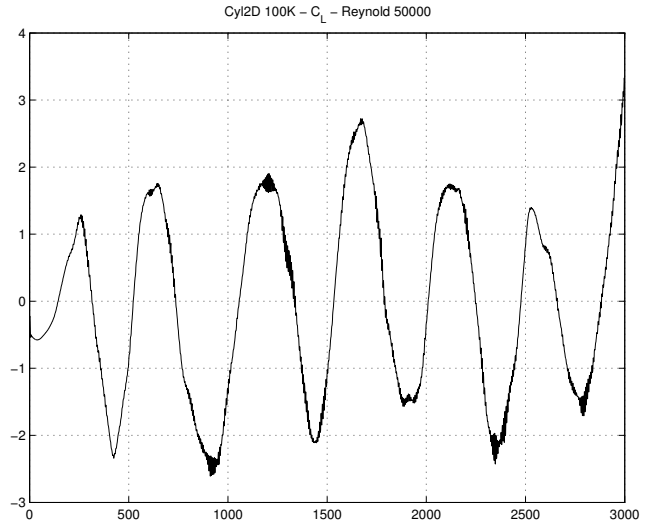

Figure 12. 2D single cylinder without shear at free stream - $Re = 50000$ - Lift coefficient (C_L).

The table included below as a summary of the results obtained for single cylinders.

Table I. Force coefficients for a single cyl. Main results. **Note**:

Case	C_L	C_D	*Strouhal*
$Re = 100$ (*Monolithic*) $K = 0$			
min	-0.3308	1.328	
max	0.3308	1.347	
mean	0	1.3375	0.1591
(*References*) [8]		≈ 1.4	≈ 0.16
(*References*) [3]	0 ± 0.35	≈ 1.38	
$Re = 200$ (*Monolithic*) $K = 0$			
min	-0.677	1.27	
max	0.677	1.362	
mean	0	1.315	0.1843
(*References*) [8]		≈ 1.4	≈ 0.19
(*References*) [3]	0 ± 0.76	≈ 1.39	
(*References*) [11]	0 ± 0.67	$\approx 1.27 \pm 0.04$	0.184
$Re = 1000$ (*Monolithic*) $K = 0$			
min	-1.35	1.23	
max	1.35	1.66	
mean	0	1.4665	0.21645
(*References*) [8]		≈ 1.2	≈ 0.21
(*References*) [3]	0 ± 1.56		
$Re = 10000$ (*Monolithic*) $K = 0$			
min	-2.0	1.1	
max	2.0	2.27	
mean	0	1.7645	
(*References*) [7]		≈ 1.125	≈ 0.2
$Re = 50000$ (*FS Scheme*) $K = 0$			
min	1.4182×10^{-1}	-2.608	
max	2.1597	3.330	
mean	-2.575×10^{-2}	1.3629	
(*References*) [7]		≈ 1.25	≈ 0.2
(*References*) [1]	-0.00 ± 0.02	1.22 ± 0.02	≈ 0.193
$Re = 50000$ (*FS Scheme*) $K = 0.05$			
mean	-4.6501×10^{-1}	1.4506	
(*References*) [1]	-0.03 ± 0.02	1.14 ± 0.02	≈ 0.188
$3D$ $Re = 50000$ (*FS Scheme*) $K = 0$			
mean	-1.8414×10^{-3}	1.1646	
(*References*) [1]	-0.00 ± 0.02	1.22 ± 0.02	≈ 0.193

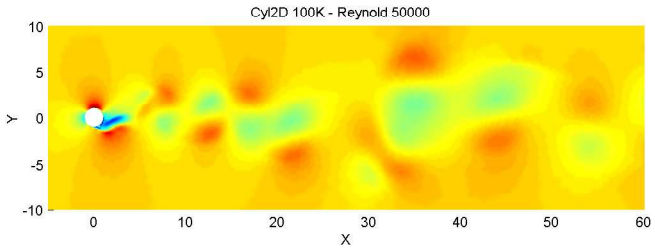

Figure 13. 2D single cylinder without shear at free stream - Axial velocity.

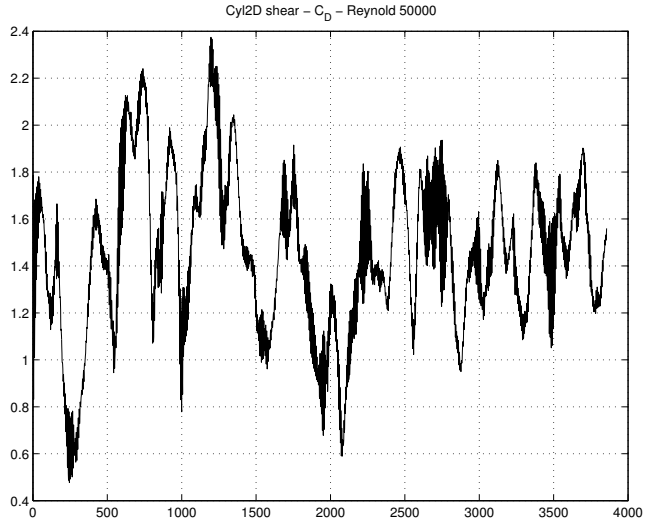

Figure 14. 2D single cylinder - $K = 0.05$ - $Re = 50000$ - Drag coefficient (C_D).

4. FLOW AROUND STAGGERED CIRCULAR CYLINDERS

This section includes a 2D flow around two circular cylinder in tandem and side by side configuration without shear flow in the free stream at a Reynolds number of 200. Next a 2D flow around two circular cylinder in tandem, side by side and 30° configuration with shear flow in the free stream at a Reynolds number of 50000 is included. Finally a table is presented to summarize the whole results.

4.1. Test # 3: Two 2D cylinders in tandem and side by side configuration without shear - $Re = 200$

Being the goal of this work to assess the influence of the interference among cylinders over the drag and lift forces this test case start showing a validation for low Reynolds number like 200. There are several references concerning with low Reynolds but not so much with high

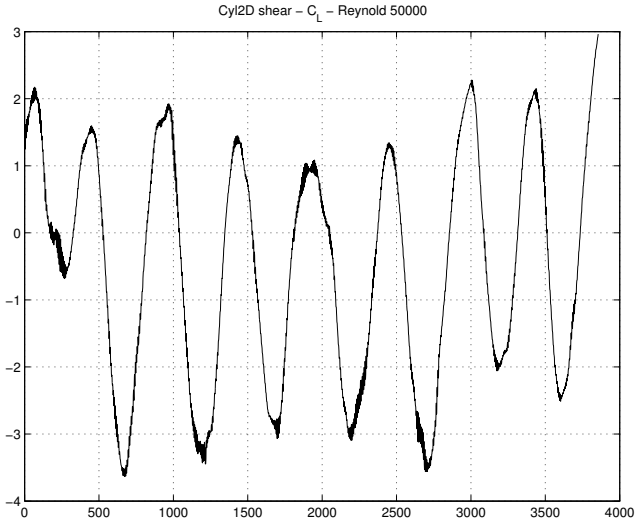

Figure 15. 2D single cylinder - $K = 0.05$ - $Re = 50000$ - Lift coefficient (C_L).

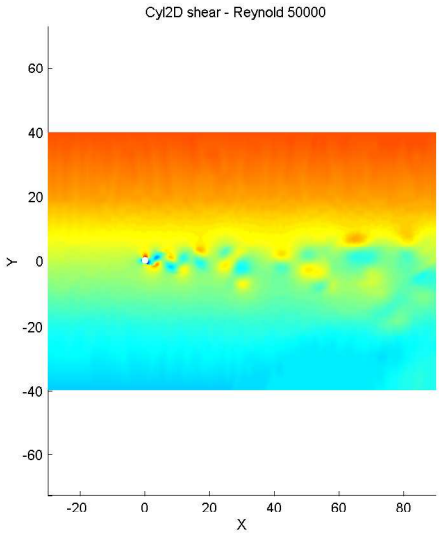

Figure 16. 2D single cylinder without shear at free stream - Axial velocity.

Reynolds number. For this example we follow the work done by Meneghini et.al. [2] where two cylinder configurations are evaluated, first a tandem and later a side by side cylinder array.

Next figures show the drag and lift time history for these two cases confirming the good agreement between the present solution against the cited bibliographic reference.

Figure17 plots the drag for the upstream cylinder (up) and downstream cylinder (down)

where it is possible to note the suction of the rear cylinder .

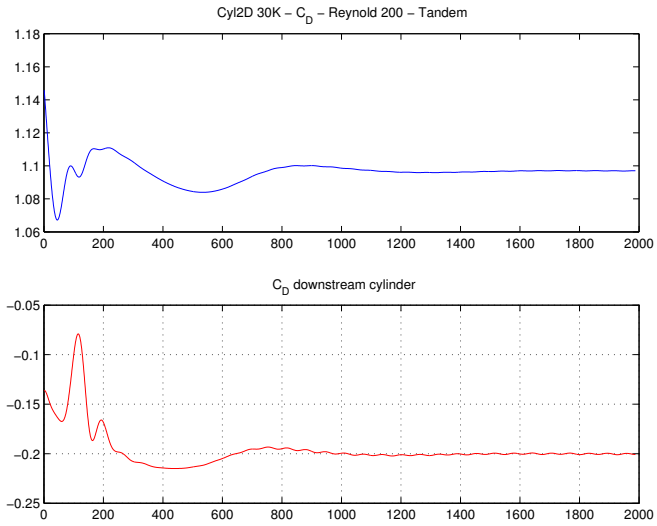

Figure 17. 2D cylinder in tandem arrangement - $Re = 200$ - Drag coefficient (C_D).

Figure18 plots the lift for both cylinder, having both cylinder a null mean lift value with a stronger amplitude for the second cylinder.

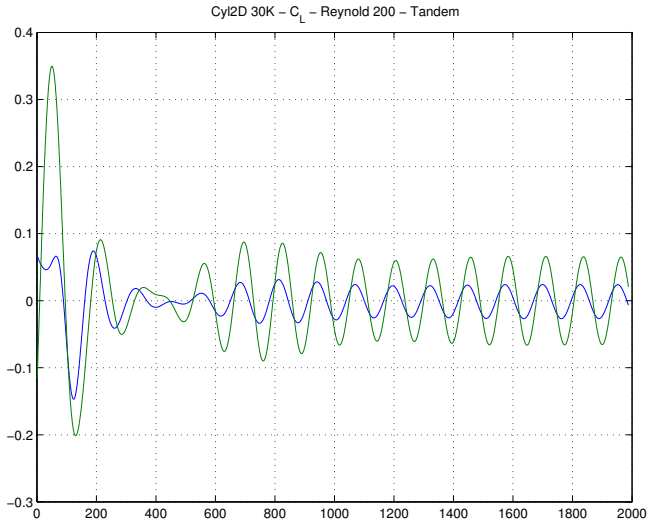

Figure 18. 2D cylinder in tandem arrangement - $Re = 200$ - Drag coefficient (C_L). (blue) : upstream , (green) : downstream

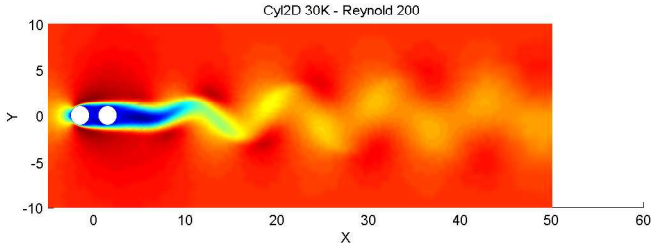

Figure 19. 2D cylinder in tandem arrangement - $Re = 200$ - x-velocity.

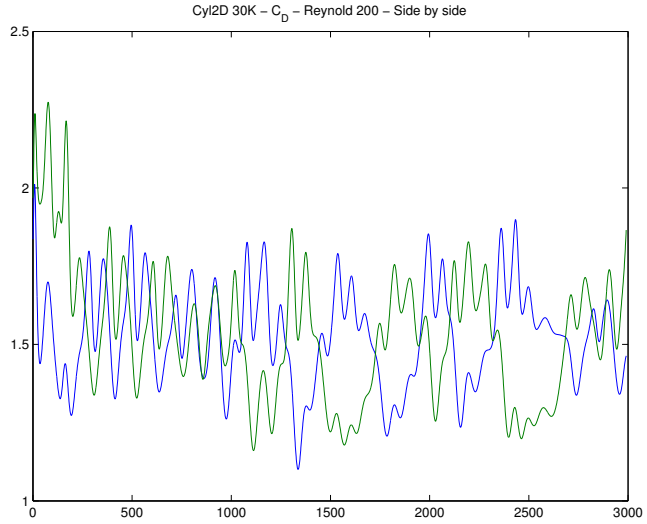

Figure 20. 2D cylinder side by side arrangement - $Re = 200$ - Drag coefficient (C_D). (blue) : upstream , (green) : downstream

4.2. Test # 4: Two 2D cylinders in tandem, side by side and 30° *configuration with shear* - $Re = 50000$

Following Akosile paper [1] in this section some circular cylinders configurations included in that reference are tested. First, the tandem configuration for the minimum pitch length between cylinder centers, next the side by side for the maximum pitch length and finally a 30° configuration for the maximum pitch length is assesed.

Results for these three test cases are included in the following figures and finally a comparative table is included to check the accuracy of the present numerical results against experimental measurements extracted from [1] paper.

$P/D = 1.125 - \alpha = 0^{\circ} - K = 0.05$

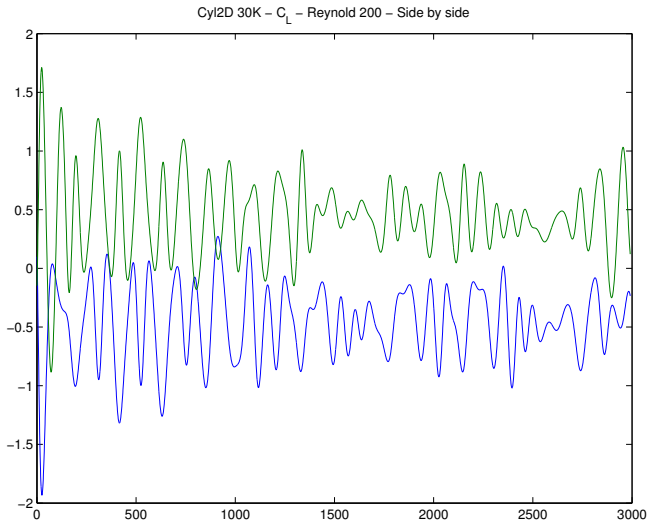

Figure 21. 2D cylinder side by side arrangement - $Re = 200$ - Drag coefficient (C_L). (blue) : upstream , (green) : downstream

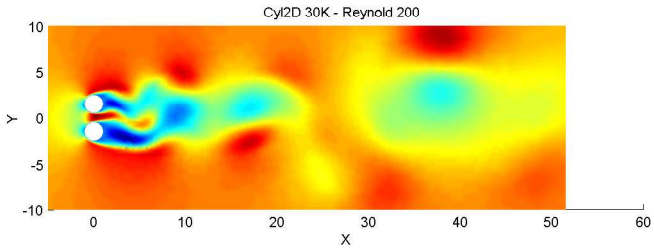

Figure 22. 2D cylinder side by side arrangement - $Re = 200$ - x-velocity.

$P/D = 1.125 - \alpha = 0^{\circ} - K = 0.05$

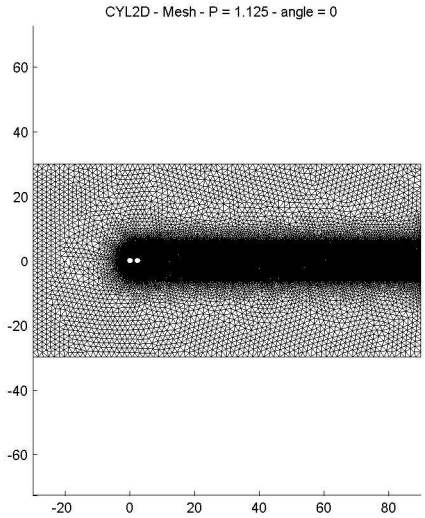

Figure 23. 2D cylinder arrangement - $Re = 50000$ - mesh.

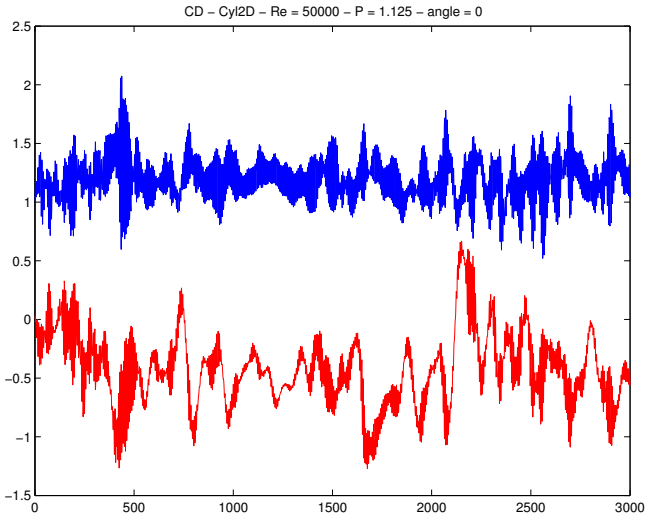

Figure 24. 2D cylinder arrangement - $Re = 50000$ - C_D. (blue) : upstream , (red) : downstream

$P/D = 1.125 - \alpha = 0^\circ - K = 0.05$

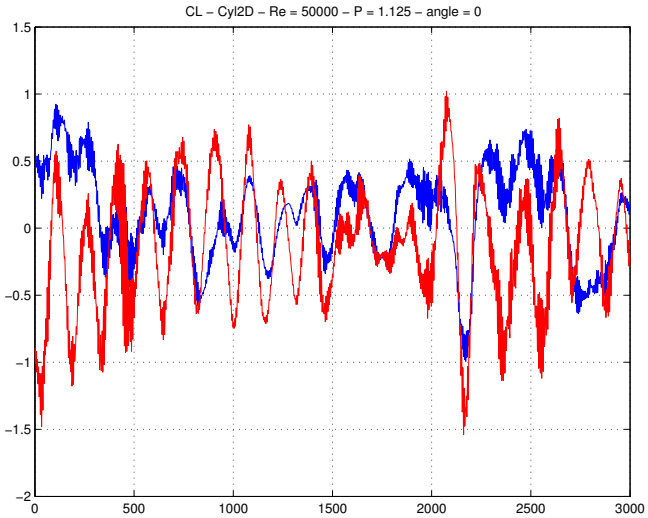

Figure 25. 2D cylinder arrangement - $Re = 50000$ - C_L. (blue) : upstream , (red) : downstream

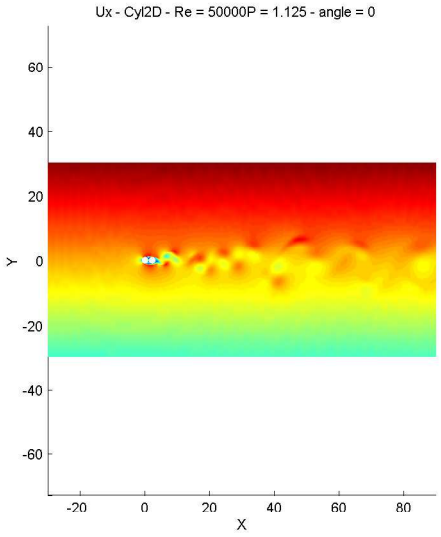

Figure 26. 2D cylinder arrangement - $Re = 50000$ - u_x.

Next table is included as a summary of the results obtained for two cylinders arrangements.

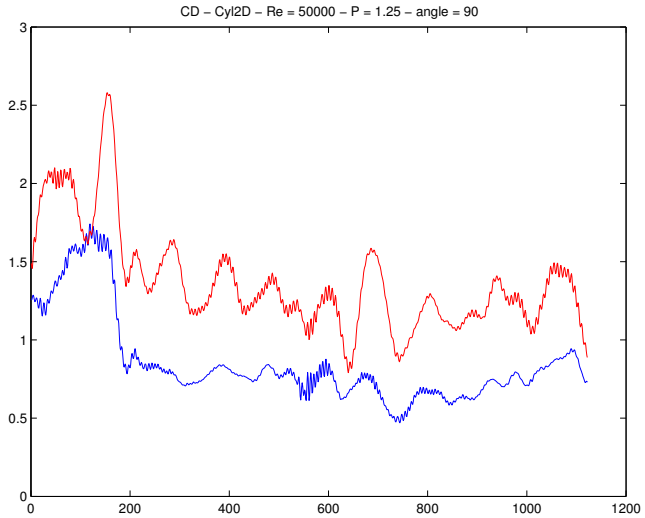

Figure 27. 2D cylinder arrangement - $Re = 50000$ - C_D. (blue) : upstream , (red) : downstream

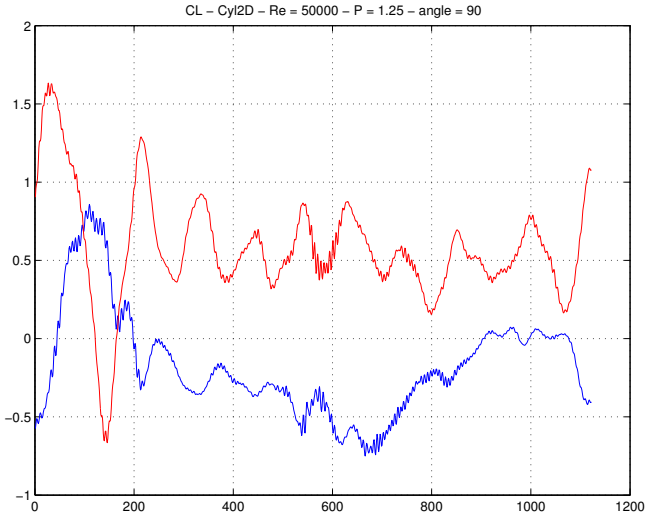

Figure 28. 2D cylinder arrangement - $Re = 50000$ - C_L. (blue) : upstream , (red) : downstream

References for tandem, side by side and $\theta = 30\circ$ cylinder arrangements in [1] are not enough clear to identify values to be included in the table above included. However the agreement is not good enough and using the arguments presented by Professor Balachandar [13] three dimensional simulations seems to be necessary to improve them.

The following figures show an spectra of vortex dynamics for the three simulations taken

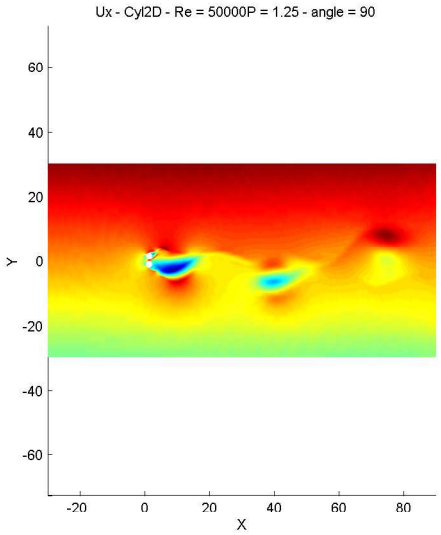

Figure 29. 2D cylinder arrangement - $Re = 50000$ - u_x.

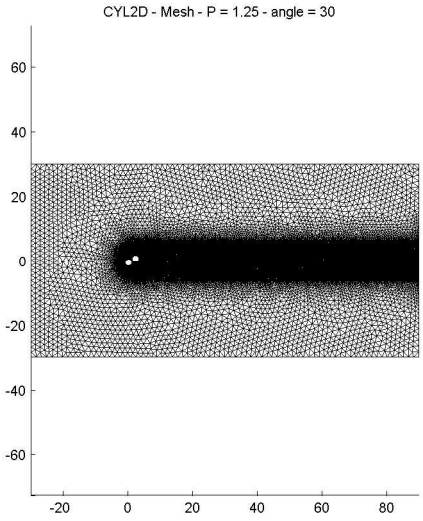

Figure 30. 2D cylinder arrangement - $Re = 50000$ - mesh.

from [1] for upstream and downstream cylinders, for C_D and C_L coefficients. These values have some similarities with those reported in [1].

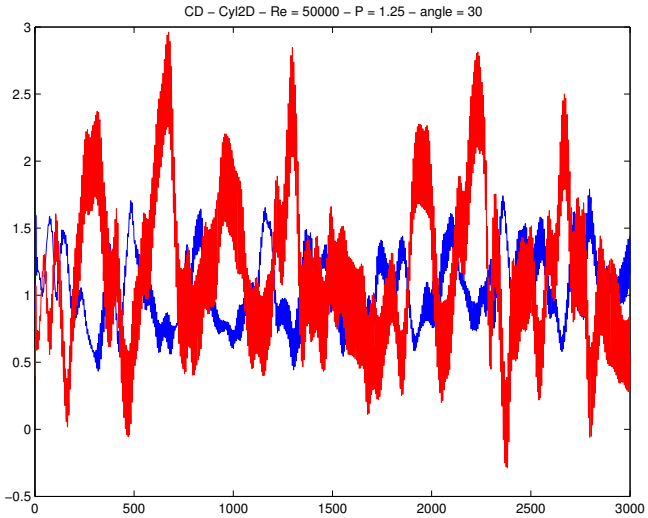

Figure 31. 2D cylinder arrangement - $Re = 50000$ - C_D. (blue) : upstream , (red) : downstream

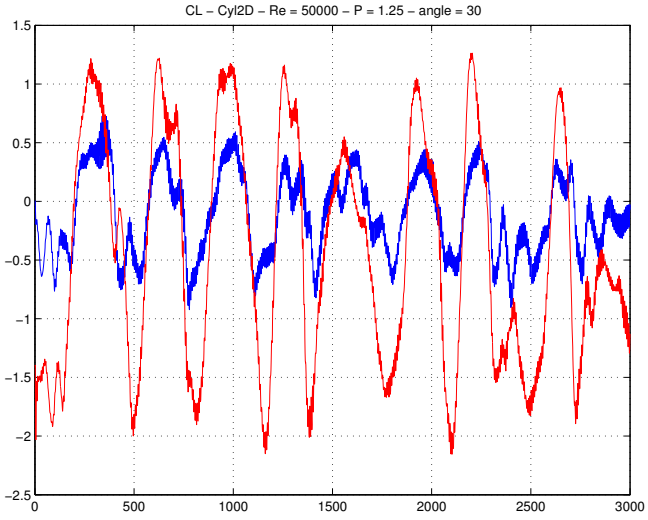

Figure 32. 2D cylinder arrangement - $Re = 50000$ - C_L. (blue) : upstream , (red) : downstream

5. 3D FLOW AROUND A SINGLE CIRCULAR CYLINDER

Finally a 3D flow around a single circular cylinder without shear flow in the free stream at a Reynolds numbers of 50000 is included. The results of this section has the goal of confirming the previously cited comments from Professor Balachandar in order to include real 3D physical effects to improve the matching of experimental results.

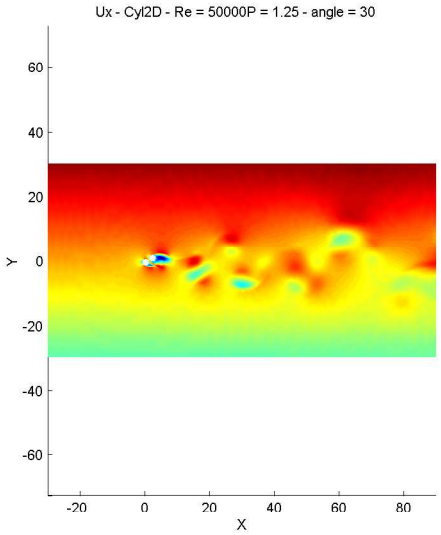

Figure 33. 2D cylinder arrangement - $Re = 50000$ - u_x.

5.1. Test # 5: Single 3D cylinder without shear at Re = 50000

Finally in order to confirm earlier published assumptions about the importance of three dimensional flow structures to influence the drag and lift forces for medium Reynolds numbers a full 3D for a finite circular cylinder was carried out. The spanwise length was chosen according to a compromise between computational resources and solution accuracy. Following [13, 6, 12] the B-mode spanwise vortex shedding has a wavelength of about the cylinder diameter, so the computational domain width was adopted of two cylinder diameters with 30 nodes in between. Starting from the 2D solution extruded in the third dimension and after a z-component velocity perturbation applied in the following way:

$$w(t) = 0.02 \times (1 - cos(2\pi t)) \;\; (0 \leq t - t_{2D} \leq 1) \tag{3}$$

where t_{2D} is the final time for the 2D simulation.

Results of 3D simulation are included in the following figures 40, 41, 42 and 43 showing an improved solution in good agreement with experimental results.

The time step used was 0.05 seconds, therefore the Strouhal number for this simulation is around 10 seconds for each period in agreement with observed experiments.

A 3D animation of this simulation is available at `http://venus.ceride.gov.ar/cimec`

6. CONCLUSIONS

Numerical experiments of several circular cylinder arrangements were performed for a medium size Reynolds number. After some validations for a single cylinder and also for two cylinders in tandem and side by side for a very low Reynolds numbers were the flow pattern is essentially 2D the extension to a Reynolds number of 50,000 showed that 2D simulations are not accurate

Table II. Force coefficients for several cyls. Main results. **Note**:

Case	C_L *upwind*	C_L *downwind*	C_D *upwind*	C_D *downwind*	*Strouhal*
$P/D = 1.125$ $Re = 50000$ (FS *Scheme*) $K = 0.05$ $\theta = 0\circ$ *mean*	1.0961×10^{-1}	-1.3013×10^{-1}	1.1900	-4.2445×10^{-1}	
($Re f erences$) [1]					
$P/D = 1.25$ $Re = 50000$ (FS *Scheme*) $K = 0.05$ $\theta = 30\circ$ *mean*	-1.1268×10^{-1}	-4.3049×10^{-1}	1.0593	1.1757	
($Re f erences$) [1]					
$P/D = 1.25$ $Re = 50000$ (FS *Scheme*) $K = 0.05$ $\theta = 90\circ$ *mean*	-1.7151×10^{-1}	5.8239×10^{-1}	8.5518×10^{-1}	1.3756	
($Re f erences$) [1]					
$P/D = 1.5$ $Re = 200$ (FS *Scheme*) $K = 0$ $\theta = 0\circ$ *mean*	-3.6137×10^{-3}	-4.6608×10^{-3}	1.1098e	-1.6132×10^{-1}	
($Re f erences$) [2]			1.06	-0.18	0.167
$P/D = 1.5$ $Re = 200$ (FS *Scheme*) $K = 0$ $\theta = 90\circ$ *mean*	-4.7116×10^{-1}	4.4515×10^{-1}	1.5429	1.5538	
($Re f erences$) [2]	-0.40	0.4	1.32	0.132	

to fit experimental measurements as was reported in earlier publications. 3D simulation for a single cylinder show a noticeable improvement in the solution for such a flow regime confirming the conclusions arrived by other authors. Therefore a 3D simulation is needed in order to capture accurately the vortex shedding structures for such a Reynolds number. Probably for very high Reynolds numbers where the flow seems to behave like two dimensional be more adequate again for 2D numerical simulation of real world physics.

REFERENCES

1. Akosile O, Sumner D. Staggered circular cylinders immersed in a uniform planar shear flow *Journal of Fluids and Structures*. 2003; **18**:613-633.
2. Meneghini J, Saltara F, Siqueira C, Ferrari J. Numerical simulation of flow interference between two circular cylinders in tandem and side by side arrangements. *Journal of Fluids and Structures*. 2001; **15**:327-350.

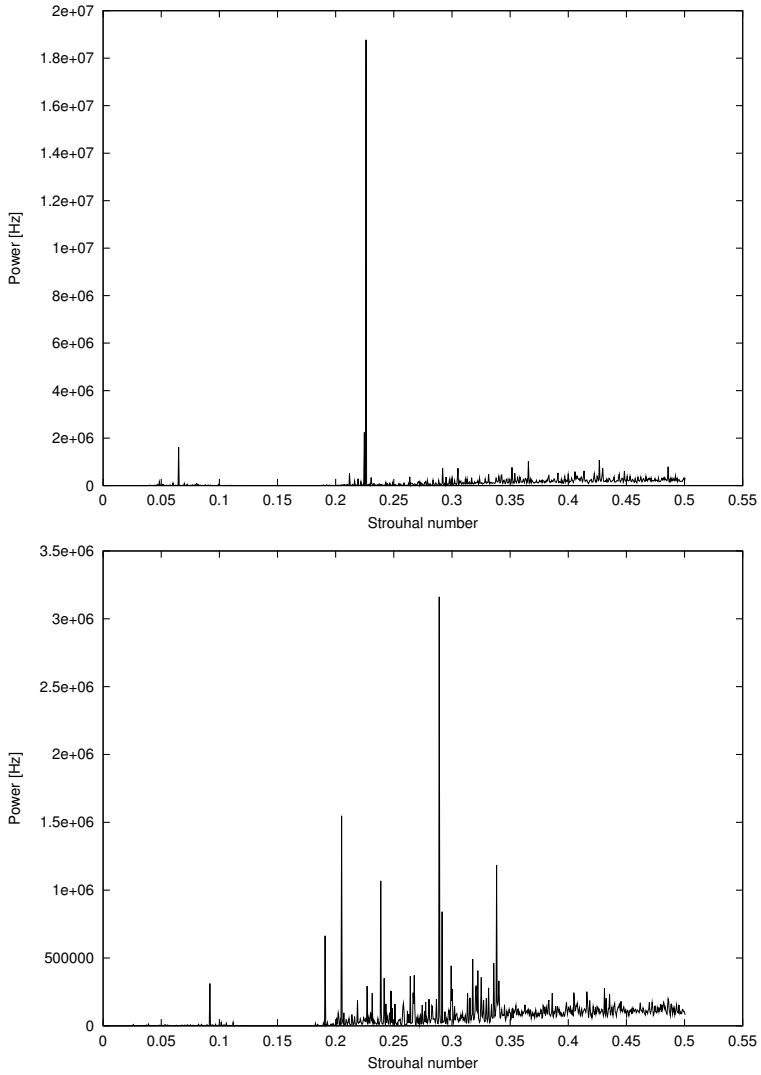

Figure 34. 2D upstream(a)/downstream(b) cylinder C_D Strouhal - $K = 0.05$ - $P/D = 1.125$ - $Re = 50000$.

3. Braza M, Chassaing P. and Ha Minh H. Numerical study and physical analysis of the pressure and velocity fields in the near wake of a circular cylinder. *Journal of Fluid Mechanics.* 1986; **164**:79-130.
4. Shih R, Tezduyar TE. Numerical experiments with the location of the downstream boundary for flow past a cylinder. *University of Minnesota Supercomputer Institute Research Report* 1990; **UMSI 90/38**.
5. Behr M, Liou J, Shih R, Tezduyar TE. Vorticity-Stream function formulation of unsteady incompressible flow past a cylinder: sensitivity of the computed flow field to the location of the downstream boundary. *University of Minnesota Supercomputer Institute Research Report* 1990; **UMSI 90/87**.
6. Kashiyama K, Tamai T, Inomata W, Yamaguchi S. A parallel finite element method for incompressible Navier-Stokes flows based on unstructured grids *Computer Methods in Applied Mechanics and*

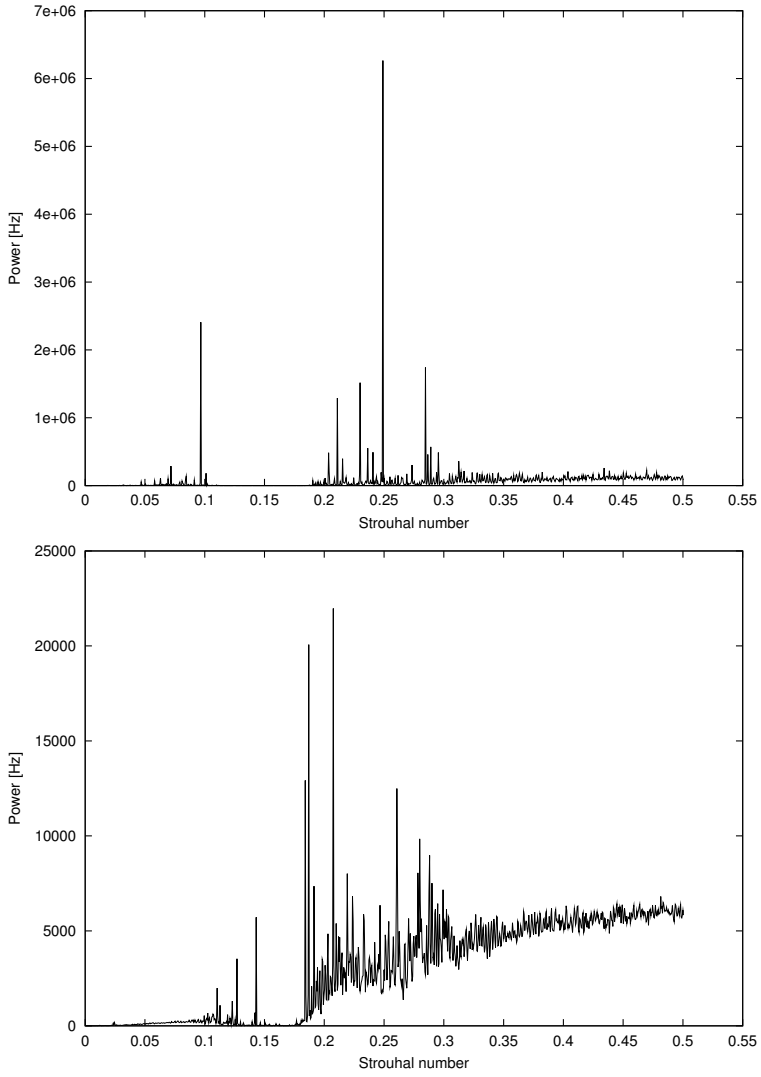

Figure 35. 2D upstream(a)/downstream(b) cylinder C_L Strouhal - $K = 0.05$ - $P/D = 1.125$ - $Re = 50000$.

Engineering. 2000; **190**:333-344.
7. Cantwell B, Coles D. An experimental study of entrainment and transport in the turbulent near wake of a circular cylinder. *Journal of Fluid Mechanics.* 1983; **136**:321-374.
8. Roshko A. Experiments on the flow past a circular cylinder at very high Reynolds number. *Journal of Fluid Mechanics.* 1961; **10**:345-356.
9. Williamson CHK. Vortex dynamics in the cylinder wake. *Annual Review of Fluid Mechanics.* 1996; **28**:477-539.
10. Tezduyar T, Mittal S, Ray S, Shih R. Incompressible flow computations with stabilized bilinear and linear equal order interpolation velocity pressure elements. *Computer Methods in Applied Mechanics and*

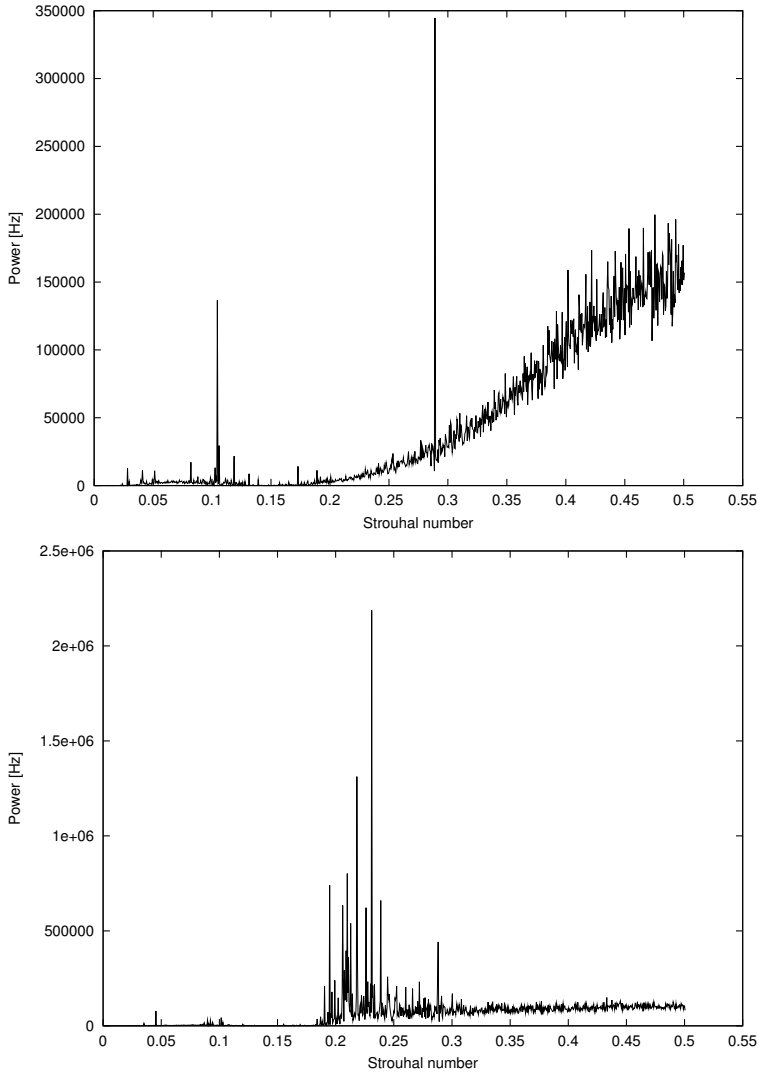

Figure 36. 2D upstream(a)/downstream(b) cylinder C_D Strouhal - $K = 0.05$ - $P/D = 1.25$ - $Re = 50000$ - $\theta = 30^\circ$.

Engineering. 1992; **95**:221-242.
11. Kiris C, Kwak D. Numerical solution of incompressible Navier-Stokes equations using a fractional-step approach *Computers and Fluids.* 2001; **30(7-8)**:777-1016.
12. Gushchin V, Kostomarov A, Matyushin P, Pavlyukova E. Direct numerical simulation of the transitional separated fluid flows around a sphere and a circular cylinder. *Journal of Wind Engineering.* 2002; **90**:341-358.
13. Mittal R, Balachandar S. Effect of three-dimensionality on the lift and drag of nominally two-dimensional cylinders. *Phys. Fluids.* 1995; **7(8)**:1841-1865.
14. Norberg C. Flow around a circular cylinder: Aspects of fluctuating lift. *Journal of Fluids and Structures.*

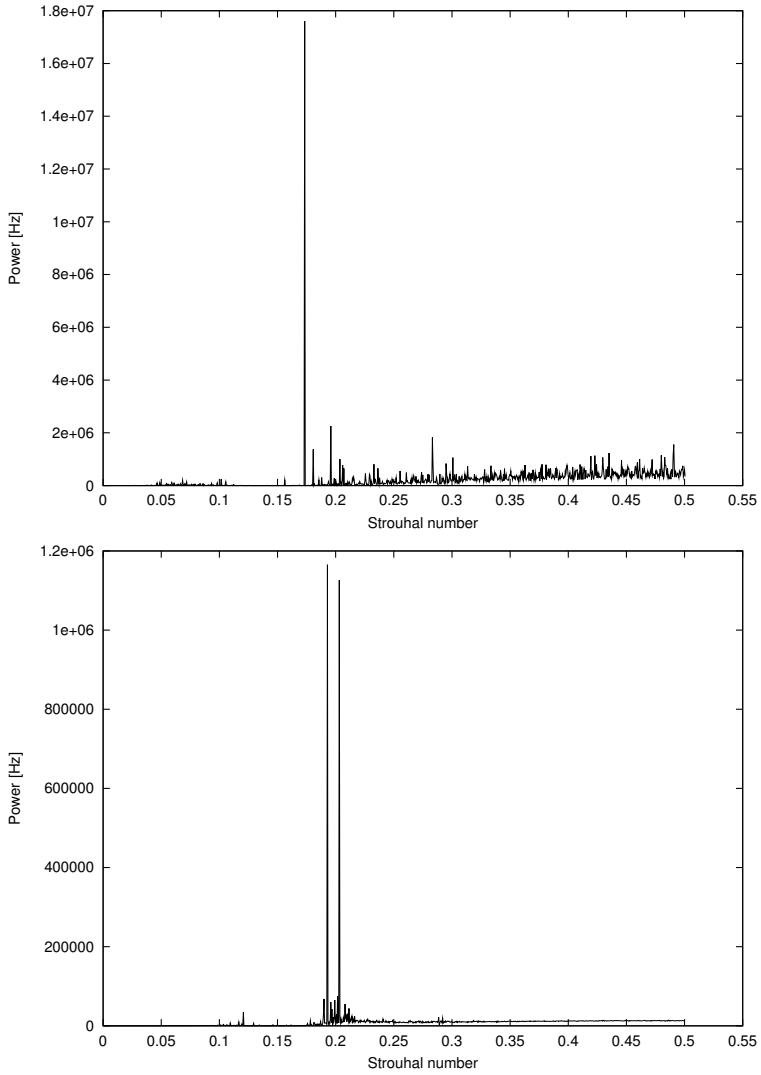

Figure 37. 2D upstream(a)/downstream(b) cylinder C_L Strouhal - $K = 0.05$ - $P/D = 1.125$ - $Re = 50000$ - $\theta = 30°$.

2001; **15**:459-469.
15. Kareem A, Kijewski T, Po-Chien Lu. Investigation of interference effects for a group of finite cylinders. *Journal of Wind Engineering.* 1998; **77 & 78**:503-520.
16. Sharman B, Lien F, Davidson L, Norberg C. Numerical predictions of low Reynolds number flows over two tandem circular cylinders. *Int. J. Num. Methods in Fluids.* 2005; **47(5)**:423-447.

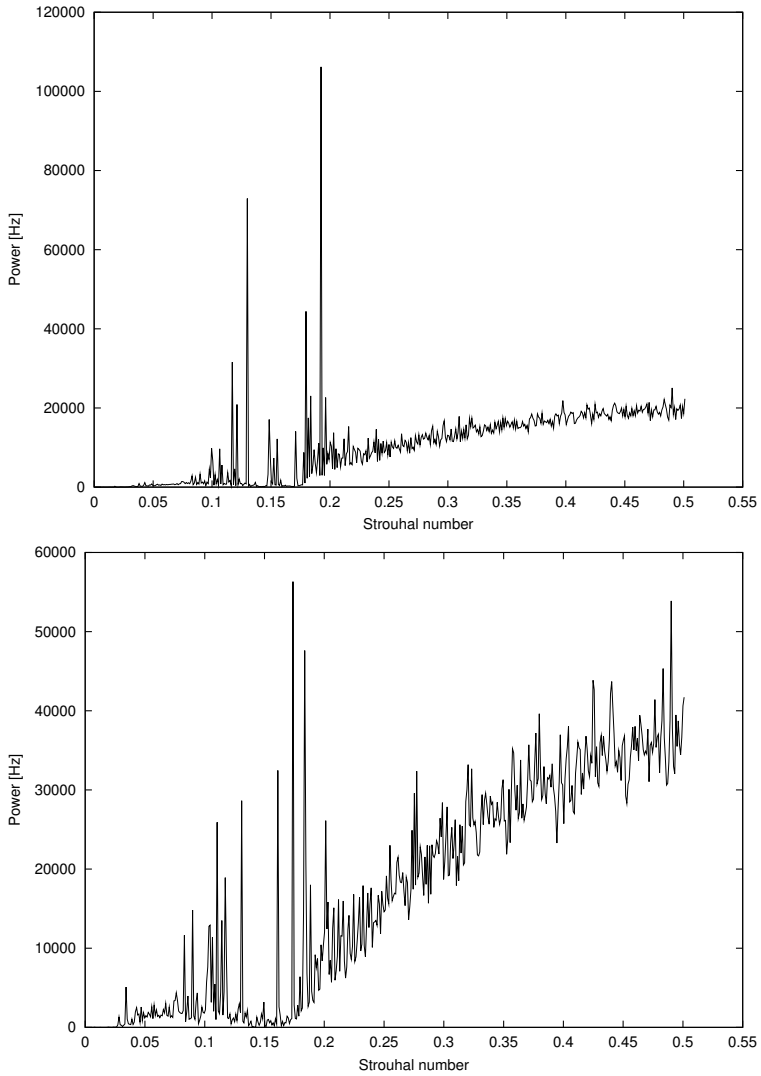

Figure 38. 2D upstream(a)/downstream(b) cylinder C_D Strouhal - $K = 0.05$ - $P/D = 1.25$ - $Re = 50000$ - $\theta = 90^\circ$.

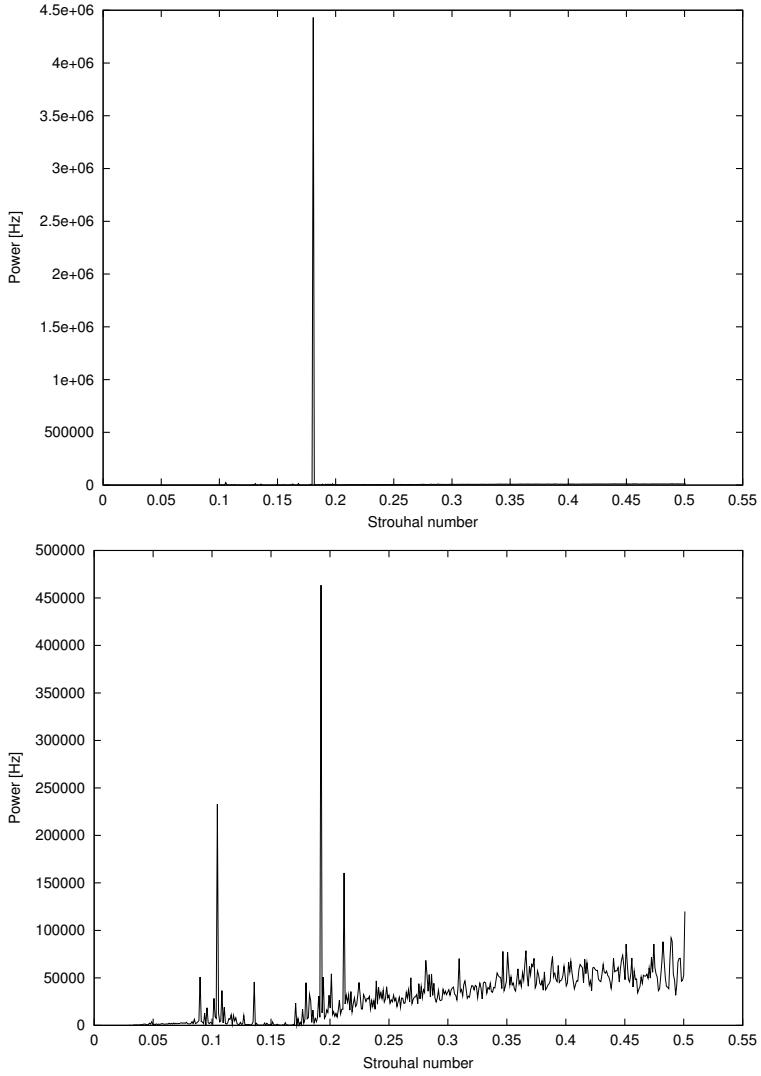

Figure 39. 2D upstream(a)/downstream(b) cylinder C_L Strouhal - $K = 0.05$ - $P/D = 1.125$ - $Re = 50000$ - $\theta = 90°$.

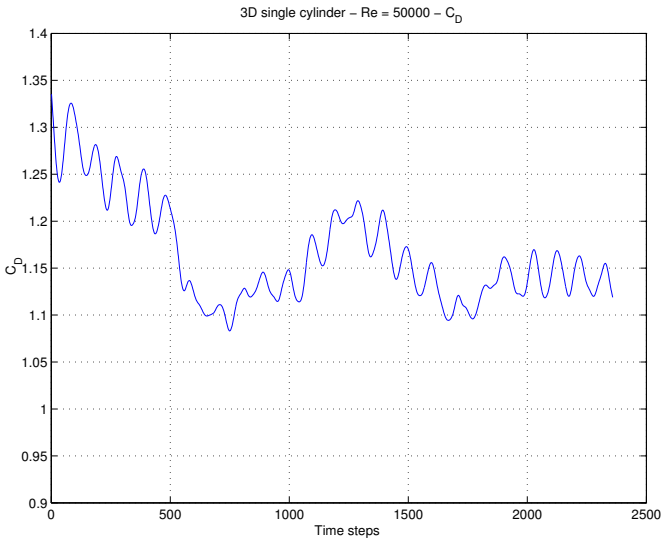

Figure 40. 3D single cylinder - $K = 0$ - $Re = 50000$ - C_D.

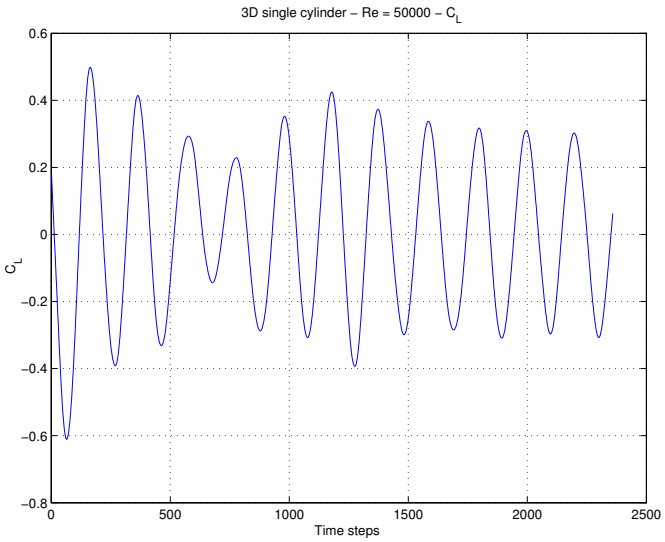

Figure 41. 3D single cylinder - $K = 0$ - $Re = 50000$ - C_L.

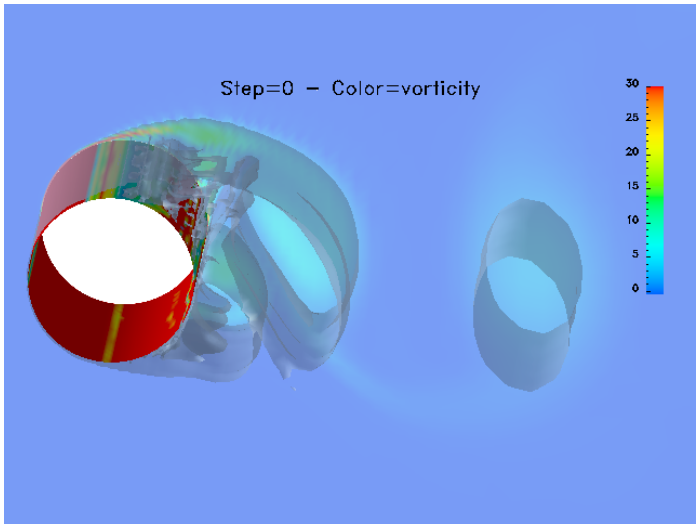

Figure 42. 3D single cylinder - $K = 0$ - $Re = 50000$ - Step 0.

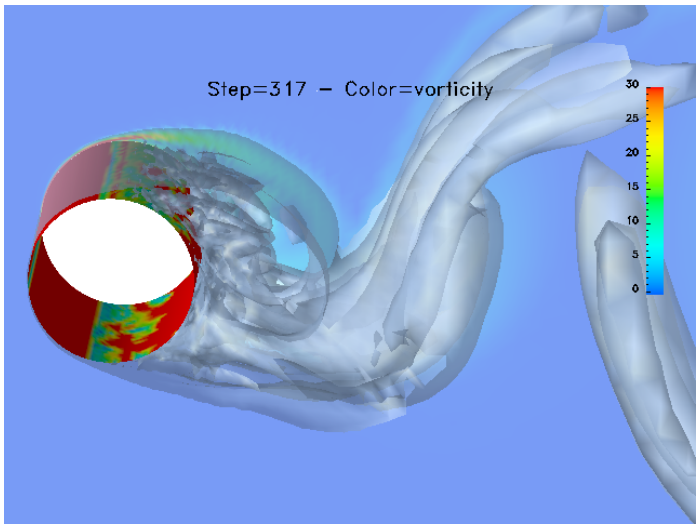

Figure 43. 3D single cylinder - $K = 0$ - $Re = 50000$ - Step 317.